

Well-Defined Calcium Initiators for Lactide Polymerization

Malcolm H. Chisholm,* Judith C. Gallucci, and Khamphée Phomphrai

Department of Chemistry, The Ohio State University, 100 West 18th Avenue, Columbus, Ohio 43210-1185

Received July 14, 2004

A series of monomeric amide or aryloxide complexes of the form LCaX , where $\text{L} = \text{CH}[\text{CMeNC}_6\text{H}_3\text{-2,6-Pr}_2^1]_2$, $\text{CH}[\text{CMeNC}_6\text{H}_4\text{-2-OMe}]_2$, a bulky tris-pyrazolyl borate, Tp^{ipr} or Tp^{ibu} or 9-BBN-pz₂ and $\text{X} = \text{N}(\text{SiMe}_3)_2$ or $\text{OC}_6\text{H}_3\text{-2,6-Pr}_2^1$, has been prepared and characterized and investigated in the ring-opening polymerizations of lactide. The compounds $(\text{Tp}^{\text{ibu}})\text{CaX}$ in THF are shown to be highly active and stereoselective. The propylene oxide complex $(\text{Tp}^{\text{ibu}})\text{Ca}(\text{OC}_6\text{H}_3\text{-2,6-Pr}_2^1)\cdot(\text{PO})$ has been isolated and structurally characterized (single-crystal X-ray) and shown to be inert to the polymerization of PO.

Introduction

New generation polymers that are biodegradable and biocompatible and are formed from readily available, inexpensive, renewable resources will gain increasing prominence in the marketplace and offer significant challenges and opportunities for chemists.¹ Polylactides (PLAs) and their copolymers and blends are one such group of new generation polymers with wide-ranging applications from bulk packaging materials to controlled release of substances and polymer scaffolds for tissue engineering.² For a bulk packaging material, a melt polymerization of lactide, LA, in the presence of a metal containing catalyst such as tin(II) octanoate provides a convenient route to PLA.³ However, this production of PLAs offers little control of molecular weight because of competing side reactions such as trans-esterification. Furthermore, it is not stereoselective and the metal catalyst remains imbedded in the polymer. The use of well-defined single-site catalyst systems, as has now been established for poly α -olefin synthesis,⁴ is an attractive possibility for the production of PLAs with specific molecular weights and microstructures. Various discrete metal complexes have been employed in lactide polymerization and these include the

metals Al, Zn, Mg, Y, Ln, Sn(II), Sn(IV), and Fe(II), and an excellent general review of the use of metal coordination complexes in PLA production appeared recently.⁵ Probably the most successful catalyst developed to date is the Coates β -diiminate complex $[(\text{BDI})\text{Zn}(\text{OPr}^i)]_2$ where BDI is $\text{CH}[\text{CMeNC}_6\text{H}_3\text{-2,6-Pr}_2^1]_2$.⁶ This shows living polymerization characteristics, is rapid at room temperature, and shows significant stereoselectivity in the production of heterotactic PLA from *rac*-LA. Hillmyer and Tolman have also recently reported a highly active zinc complex that holds promise for future development.⁷ We are attracted to the use of calcium in PLA production. Calcium is inexpensive, biocompatible, and a kinetically labile ion.⁸ It is hard, like the Mg^{2+} ion, but significantly larger than either Mg^{2+} or the softer Zn^{2+} ion.⁹ Calcium finds extensive industrial use in the production of polyoxygenates such as poly(ethylene oxide), PEO, and polypropylene oxide, PPO.¹⁰ Could calcium similarly find use in the production of PLAs? A few examples of calcium complexes being used in PLA production have appeared in the literature but none of these have

* Author to whom correspondence should be addressed. E-mail: chisholm@chemistry.ohio-state.edu.

(1) Ritter, S. K. *Chem. Eng. News* **2002**, 80 (July 1st), 26.

(2) (a) Gilding, D. K.; Reed, A. M. *Polymer* **1979**, 20, 1459. (b) Lewis, D. H. In *Biodegradable Polymers as Drug Delivery Systems*; Chasin, M., Langer, R., Eds.; Marcel Dekker: New York, 1990; p 1. (c) Mooney, D. J.; Organ, G.; Vacanti, J. P.; Langer, R. *Cell Transpl.* **1994**, 2, 203.

(3) Kowalski, A.; Duda, A.; Penczek, S. *Macromolecules* **2000**, 33, 689–695.

(4) For a recent review see Coates, G. W. *Chem. Rev.* **2000**, 100, 1223–1252.

(5) For a recent review see O'Keefe, B. J.; Hillmyer, M. A.; Tolman, W. B. *J. Chem. Soc., Dalton Trans.* **2001**, 2215–2224.

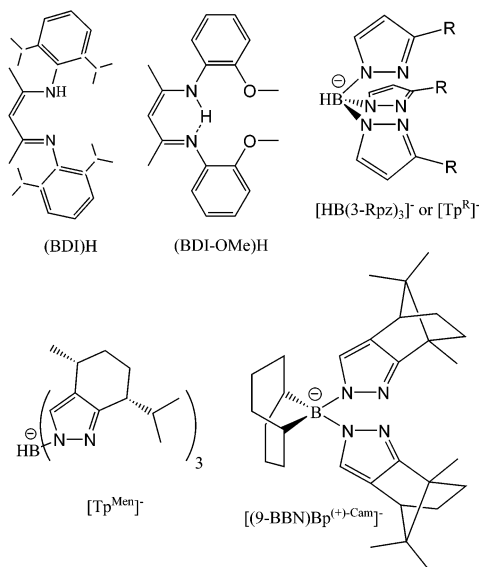
(6) Chamberlain, B. M.; Cheng, M.; Moore, D. R.; Ovitt, T. M.; Lobkovsky, E. B.; Coates, G. W. *J. Am. Chem. Soc.* **2001**, 123, 3229–3238.

(7) William, C. K.; Breyfogle, L. E.; Choi, S. K.; Nam, W.; Young, V. G., Jr.; Hillmyer, M. A.; Tolman, W. B. *J. Am. Chem. Soc.* **2003**, 125, 11350–11359.

(8) Voet, D.; Voet, J. G. In *Biochemistry*, 2nd ed.; John Wiley & Sons: New York, 1995; pp 500–502, 1246–1250, 1265–1267.

(9) Huheey, J. E.; Keiter, E. A.; Keiter, R. L. In *Inorganic Chemistry: Principles of Structure and Reactivity*, 4th ed.; Harper Collins College Publishers: New York, 1993; pp 292, 344–348.

(10) Goeke, G. L.; Park, K.; Karol, P. J.; Mead, B. U.S. Patent 4,193,892, 1980.

Scheme 1. Representations of the Ligands Employed in This Work and Their Abbreviations

employed discrete well-defined complexes.¹¹ We describe here our initial foray into the development of well-defined calcium initiators of the type LCaX for the production of PLAs. The selection of ligands L employed in this study is shown in Scheme 1.

This selection allows a direct comparison with earlier studies involving magnesium and zinc and the introduction of the β -diiminate CH[CMenC₆H₄-2-OMe]₂ (BDI-OMe) affords additional coordination to the large calcium metal via the ether groups. The use of the chiral Tp ligand affords the potential for stereoselective polymerizations via enantiomorphic site control. A preliminary account of some of these findings has appeared.¹²

Results and Discussion

Syntheses. The syntheses of calcium–amide or alkoxide complexes of the type LMX, where X = OR or NR₂, by metathetic reactions employing alkali metals provides a challenge since it is not clear when a reaction will proceed and if so, which groups will exchange. As starting calcium compounds, we employed CaI₂ which is sparingly soluble in THF and has the lowest lattice energy of any calcium halide and Ca(N(SiMe₃)₂)₂ which is susceptible to exchange reactions via proton transfer to the amide.

(BDI)CaN(SiMe₃)₂·(THF), 1. The β -diiminate ligand CH[CMen-(2,6-ⁱPr₂C₆H₃)₂] (BDI) can be easily attached to Zn and Mg from the reaction between (BDI)H and zinc or magnesium amides.¹³ Attempts to use a similar approach with either Ca[N(SiMe₃)₂]₂·2THF or CaH₂ were not successful. The best preparation involved a reaction of 2 equiv KN-

(SiMe₃)₂ with 1 equiv (BDI)H in THF, followed by addition of the mixture to CaI₂. This gave the moisture-sensitive compound (BDI)CaN(SiMe₃)₂·(THF), **1**, in high yield after work up. The reaction of 2 equiv (BDI)K (generated in situ) with CaI₂ in THF gave (BDI)₂Ca, **2**. The reaction of the amide complex **1** with simple alcohols such as HOⁱPr and HO^tBu resulted in the formation of various species with compound **2** as a major product. The THF in compound **1** can be removed by heating at 150 °C under vacuum for 40 min giving (BDI)CaN(SiMe₃)₂.

[HB(3-^tBupz)₃]CaN(SiMe₃)₂, 3. The synthesis of this tris-(pyrazolyl)borate calcium complex proved to be very challenging. Attempts to follow a preparation similar to that for the zinc and magnesium analogues through [HB(3-^tBupz)₃]MCl were not successful. The treatment of [HB(3-^tBupz)₃]K with CaI₂ under various organic solvents did not give [HB(3-^tBupz)₃]CaI·(THF) but seemingly several complexes, as yet unidentified, based on ¹H NMR spectroscopy. However, a slow addition of [HB(3-^tBupz)₃]Ti to CaI₂ in THF gave the desired product [HB(3-^tBupz)₃]CaI·(THF), **4**. When complex **4** was allowed to react with KN(SiMe₃)₂, a mixture of 80% [HB(3-^tBupz)₃]CaN(SiMe₃)₂, **3**, and 20% [HB(3-^tBupz)₃]K was obtained. The minor product came from the inverse metathesis of ligands. A similar problem was seen earlier in the reaction between [HB(3-^tBupz)₃]ZnCl with KO^tBu which gave [HB(3-^tBupz)₃]K.¹⁴ A very simple but most effective method to synthesize **3**, however, was from the addition of THF to a solid mixture of [HB(3-^tBupz)₃]K, CaI₂, and KN(SiMe₃)₂. This convenient one-step three-component reaction was complete overnight (> 8 h) and the product **3** was easily isolated in moderate yield. Syntheses similar to that employed for [HB(3-^tBupz)₃]CaN(SiMe₃)₂ were used in the preparations of related tris(pyrazolyl)borate calcium amide complexes. Attempts to make [HB(3-^tBupz)₃]₂Ca from the reaction of 2 equiv [HB(3-^tBupz)₃]Ti and CaI₂ failed, giving only compound **4** as a well-defined complex.

[HB(3-^tBupz)₃]Ca(O-2,6-ⁱPr₂C₆H₃)·(THF), 5. The reaction of compound **3** with 2,6-diisopropylphenol in THF gave a moisture-sensitive compound **5** in high yield. When **5** was heated to 150 °C under vacuum, THF was liberated giving [HB(3-^tBupz)₃]Ca(O-2,6-ⁱPr₂C₆H₃), **6**, in quantitative yield.

[HB(3-ⁱPrpz)₃]CaN(SiMe₃)₂·(THF), 7. The addition of THF to a mixture of [HB(3-ⁱPrpz)₃]K, CaI₂ and KN(SiMe₃)₂ after workup gave the moisture-sensitive compound **7**.

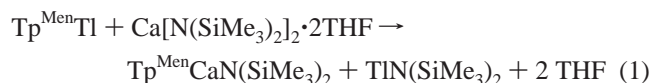
[HB(3-Phpz)₃]₂Ca, 8. Attempts to prepare [HB(3-Phpz)₃]CaN(SiMe₃)₂ failed. When the ligand L does not possess sufficient bulk, a process similar to the Schlenk equilibrium takes place to form the complex L₂Ca. In this case, the compound [HB(3-Phpz)₃]₂Ca, **8**, was produced exclusively. Even though the phenyl groups are bulky, they are planar, and may orient themselves parallel to one another giving enough room to put two ligands on one calcium ion.

[HB((7R)-ⁱPr-(4R)-Me-4,5,6,7-tetrahydro-2H-indazolyl)₃]CaN(SiMe₃)₂, 9. The ligand framework in compound **9** is

- (11) (a) Dobrzynski, P.; Kasperczyk, J.; Bero, M. *Macromolecules* **1999**, *32*, 4735–4737. (b) Li, S. M.; Rashkov, I.; Espartero, J. L.; Manolova, N.; Vert, M. *Macromolecules* **1996**, *29*, 57–62.
- (12) Chisholm, M. H.; Gallucci, J.; Phomphrai, K. *Chem. Commun.* **2003**, 48–49.
- (13) (a) Chisholm, M. H.; Gallucci, J.; Phomphrai, K. *Inorg. Chem.* **2002**, *41*, 2785–2794. (b) Chamberlain, B. M.; Cheng, M.; Moore, D. R.; Oviatt, T. M.; Lobkovsky, E. B.; Coates, G. W. *J. Am. Chem. Soc.* **2001**, *123*, 3229–3238.

- (14) Chisholm, M. H.; Eilerts, N. W.; Huffman, J. C.; Iyer, S. S.; Pacold, M.; Phomphrai, K. *J. Am. Chem. Soc.* **2000**, *122*, 11845–11854.

abbreviated as Tp^{Men} . Attempts to use an approach similar to that employed in the synthesis of **3** by starting with $\text{Tp}^{\text{Men}}\text{K}$, CaI_2 , and $\text{KN}(\text{SiMe}_3)_2$ were not successful. The reaction of $\text{Tp}^{\text{Men}}\text{Ti}$ with CaI_2 gave $\text{Tp}^{\text{Men}}\text{CaI} \cdot (\text{THF})$, **10**. However, the reaction of **10** with $\text{KN}(\text{SiMe}_3)_2$ failed to produce the title compound **9**. Nonetheless, it was found that the complex $\text{Tp}^{\text{Men}}\text{Ti}$ reacted with $\text{Ca}[\text{N}(\text{SiMe}_3)_2]_2 \cdot 2\text{THF}$ in benzene to give $\text{Tp}^{\text{Men}}\text{CaN}(\text{SiMe}_3)_2$, **9**, exclusively as illustrated in eq 1.



$\text{TiN}(\text{SiMe}_3)_2$ was removed by sublimation, giving the moisture-sensitive compound **9**. This new approach for the synthesis of a tris(pyrazolyl)borate calcium amide complex is not limited to the synthesis of **9**. The reaction between $[\text{HB}(3\text{-}^i\text{Bupz})_3]\text{Ti}$ and $\text{Ca}[\text{N}(\text{SiMe}_3)_2]_2 \cdot 2\text{THF}$ in benzene gave exclusively $[\text{HB}(3\text{-}^i\text{Bupz})_3]\text{CaN}(\text{SiMe}_3)_2$, **3**.

$[(\text{Cyclooctane-1,5-diyl})\text{bis}[(4\text{S},7\text{R})\text{-}7,8,8\text{-trimethyl-4,5,6,7-tetrahydro-4,7-methano-2H-indazol-2-yl}]\text{borato}]\text{CaN}(\text{SiMe}_3)_2 \cdot 2\text{THF}$ or $[(9\text{-BBN})\text{Bp}^{(+)-\text{Cam}}]\text{CaN}(\text{SiMe}_3)_2 \cdot 2\text{THF}$, **11**. Compound **11** can be synthesized using a preparation similar to that employed in the synthesis of compounds **3** and **7**, but with $[(9\text{-BBN})\text{Bp}^{(+)-\text{Cam}}]\text{K}$, CaI_2 and $\text{KN}(\text{SiMe}_3)_2$ as starting materials

$(\text{BDI-OMe})\text{CaN}(\text{SiMe}_3)_2 \cdot (\text{THF})$, **12** and $(\text{BDI-OMe})_2\text{Ca}$, **13**. A slow addition of 1 equiv of the free ligand $(\text{BDI-OMe})\text{H}$ into a solution of $\text{Ca}[\text{N}(\text{SiMe}_3)_2]_2 \cdot 2\text{THF}$ gave compound **12**. When 2 equiv of $(\text{BDI-OMe})\text{H}$ were used, the compound **13** was obtained in high yield. Attempts to react HO^iPr or HO^tBu with compound **12** gave compound **13** and presumably a calcium alkoxide by disproportionation.

$(\text{Tp}^{\text{But}})\text{Ca}(\text{OC}_6\text{H}_3\text{-}2,6\text{-Pr}_2^i)(\text{PO})$, **14**. The compound **6** reversibly coordinates propylene oxide, PO, and crystals of the title compounds **14** were obtained by careful crystallization in the presence of an excess of *rac*-PO.

Single Crystal and Molecular Structures. (BDI)CaN(SiMe₃)₂·(THF), 1. An ORTEP drawing of the molecular structure of the monomeric compound **1** is given in Figure 1 along with selected bond distances (Å) and angles (deg) in Table 1. The calcium atom is four-coordinate assuming a distorted tetrahedral geometry. In general, **1** has certain structural similarities to the related compounds $(\text{BDI})\text{ZnN}(\text{SiMe}_3)_2$ and $(\text{BDI})\text{MgN}(\text{SiMe}_3)_2$.¹⁵ However, calcium is larger than magnesium and zinc and is also ligated by THF; the Ca–N bond distances (2.361(1) Å) are notably longer. The NCCCN central unit of the β -diiminato ligand is almost planar as a result of π -electron delocalization, as commonly seen in β -diiminato complexes. However, the six-membered CaNCCCN ring is highly puckered where the calcium atom is 1.238(1) Å above a plane defined by N1, C2, and N2. This is an inevitable outcome when the metal is larger than

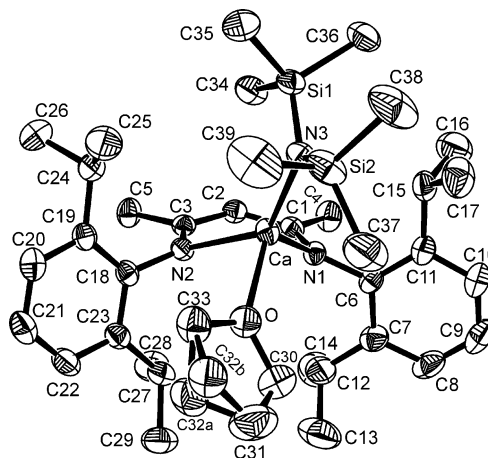


Figure 1. ORTEP drawing of the $(\text{BDI})\text{CaN}(\text{SiMe}_3)_2 \cdot (\text{THF})$ molecule with thermal ellipsoids drawn at 50% probability level. Hydrogen atoms are omitted for clarity. THF molecule is disordered at C32a and C32b.

the pocket of the ligand, and was seen in the recently reported structures of the series $(\text{BDI})_2\text{M}$ where $\text{M} = \text{Ca}$, Sr , and Ba .¹⁶

$(\text{BDI})_2\text{Ca}$, **2**. An ORTEP drawing of the molecular structure of **2** is given in Figure 2, and selected bond distances (Å) and angles (deg) are provided in Table 1. Compound **2** is monomeric and the calcium atom is four-coordinate assuming a distorted tetrahedral geometry. The arrangement of the ligand is similar to that in **1**. The six-membered CaNCCCN ring is highly puckered where the calcium atom is 1.309(1) Å above a plane defined by N1, C2, and N2. This structure determination is comparable to that reported by Harder.¹⁶

$[\eta^3\text{-HB}(3\text{-}^i\text{Prpz})_3]\text{CaN}(\text{SiMe}_3)_2 \cdot (\text{THF})$, **7**. An ORTEP drawing of the molecular structure of **7** is given in Figure 3, and selected bond distances and angles are given in Table 1. Even though the quality of the single-crystal X-ray structure is poor, some qualitative information can be extracted. Compound **7** has a monomeric structure where the calcium atom is five-coordinate assuming a trigonal bipyramidal geometry. The THF binds to calcium at an axial position and the amide binds at an equatorial position. The tridentate ligand binds to calcium via two equatorial sites and one axial site. The two methyl groups (e.g., C11 and C11*) of the isopropyl groups orient in a way to minimize repulsion by pointing themselves away from the metal core.

$[\eta^3\text{-HB}(3\text{-}^i\text{Bupz})_3]\text{Ca}(\text{O-}2,6\text{-}^i\text{Pr}_2\text{C}_6\text{H}_3)$, **6**. An ORTEP drawing of the molecular structure of **6** is given in Figure 4 along with selected bond distances (Å) and angles (deg) in Table 1. Compound **6** has a monomeric structure where the calcium atom is four-coordinate assuming a distorted tetrahedral geometry. Unlike the arrangement in **7**, all three pyrazolyl groups bind to calcium similarly. The B, Ca, and O atoms are almost collinear, $170.61(5)^\circ$, and the Ca–O bond distance is 2.106(1) Å. The average Ca–N bond distances are 2.425(1) Å and the Ca–O–C22 angle is $174.4(1)^\circ$.

$(\text{BDI-OMe})_2\text{Ca}$, **13**. An ORTEP drawing of the molecular structure of **13** is given in Figure 5, and selected bond

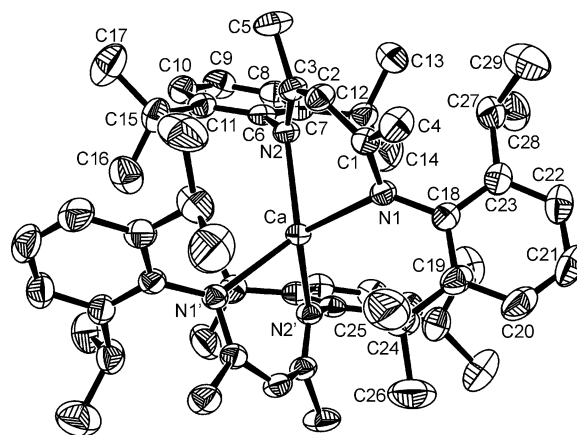
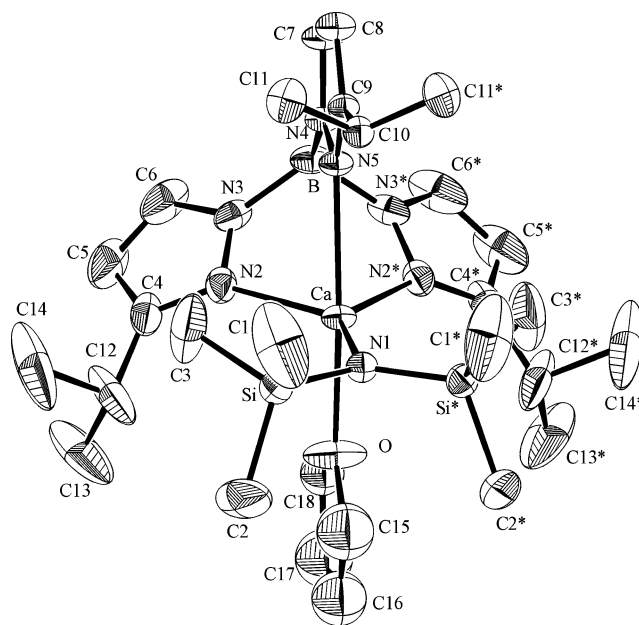
(15) Cheng, M.; Moore, D. R.; Reczek, J. J.; Chamberlain, B. M.; Lobkovsky, E. B.; Coates, G. W. *J. Am. Chem. Soc.* **2001**, *123*, 8738–8749.

(16) Harder, S. *Organometallics* **2002**, *21*, 3782.

Table 1. Selected Bond Distances (Å) and Angles (deg) for Compounds **1**, **2**, **6**, **7**, **13**, and **14**

(BDI)CaN(SiMe ₃) ₂ ·(THF), 1			
Ca–N3	2.313(1)	Ca–N2	2.370(1)
Ca–N1	2.352(1)	Ca–O	2.359(1)
N3–Ca–N1	124.79(5)	N3–Ca–O	104.88(5)
N1–Ca–O	113.79(5)	N3–Ca–N2	136.78(5)
N1–Ca–N2	81.14(5)	O–Ca–N2	91.25(5)
(BDI) ₂ Ca, 2			
Ca–N2	2.377(1)	Ca–N1	2.384(1)
N2'–Ca–N2	123.63(6)	N2'–Ca–N1	123.26(4)
N2–Ca–N1	83.08(4)	N2'–Ca–N1'	83.08(4)
N2–Ca–N1'	123.27(4)	N1–Ca–N1'	126.12(6)
Tp ^{tBu} Ca(O-2,6- ⁱ Pr ₂ C ₆ H ₃), 6			
Ca–O	2.106(1)	Ca–N5	2.412(1)
Ca–N3	2.426(1)	Ca–N1	2.437(1)
O–Ca–N5	136.79(4)	O–Ca–N3	132.31(4)
N5–Ca–N3	79.84(4)	O–Ca–N1	120.48(4)
N5–Ca–N1	85.43(4)	N3–Ca–N1	84.22(4)
C22–O–Ca	174.4(1)		
Tp ^{iPr} CaN(SiMe ₃) ₂ ·(THF), 7			
Ca–O	2.378(3)	Ca–N1	2.339(3)
Ca–N2	2.494(3)	Ca–N5	2.464(3)
N1–Ca–N2	139.84(6)	N1–Ca–O	92.3(1)
N1–Ca–N5	104.3(1)	N2–Ca–O	86.15(8)
N2–Ca–N5	81.19(8)	N2–Ca–N2*	80.2(1)
N5–Ca–O	163.4(1)		
(CH[CMcNC ₆ H ₄ -2-OMe] ₂) ₂ Ca, 13			
Ca–N1	2.503(2)	Ca–N2	2.462(2)
Ca–N3	2.486(2)	Ca–N4	2.502(2)
Ca–O1	2.586(2)	Ca–O2	2.570(2)
Ca–O3	2.534(2)	Ca–O4	2.600(2)
N2–Ca–N3	126.96(6)	N2–Ca–N4	127.14(6)
N3–Ca–N4	72.80(6)	N2–Ca–N1	71.80(6)
N3–Ca–N1	131.31(6)	N4–Ca–N1	136.74(6)
O3–Ca–O2	86.49(5)	O3–Ca–O1	97.88(5)
O2–Ca–O1	162.53(5)	O3–Ca–O4	161.34(5)
O2–Ca–O4	102.63(5)	O1–Ca–O4	78.34(5)
N2–Ca–O3	78.56(6)	N3–Ca–O3	64.08(5)
N4–Ca–O3	136.49(6)	N1–Ca–O3	80.61(6)
N2–Ca–O2	63.63(6)	N3–Ca–O2	77.23(6)
N4–Ca–O2	78.46(6)	C2–O1–Ca	114.1(1)
N1–Ca–O2	135.22(6)	C16–O2–C17	116.5(2)
N2–Ca–O1	133.78(6)	C16–O2–Ca	113.8(1)
N3–Ca–O1	89.41(6)	C8–N1–Ca	124.5(2)
N4–Ca–O1	86.91(6)	C7–N1–Ca	114.5(1)
N1–Ca–O1	62.25(5)	C10–N2–Ca	124.0(2)
N2–Ca–O4	90.82(6)	C11–N2–Ca	115.1(1)
N3–Ca–O4	133.49(6)	N1–C8–C9	123.0(2)
N4–Ca–O4	61.98(5)	C10–C9–C8	28.7(2)
N1–Ca–O4	81.52(6)	N2–C10–C9	123.7(2)
C2–O1–C1	116.2(2)	N2–C10–C19	121.3(2)
Tp ^{tBu} Ca(O-2,6- ⁱ Pr ₂ C ₆ H ₃)·(PO), 14			
Ca–O1	2.454(2)	Ca–O2	2.124(1)
Ca–N1	2.435(2)	Ca–N6	2.476(2)
Ca–N4	2.507(2)	O2–Ca–N1	119.44(6)
O2–Ca–O1	101.56(6)	N1–Ca–O1	82.13(6)
O2–Ca–N6	144.87(6)	N1–Ca–N6	95.38(6)
O1–Ca–N6	77.18(6)	O2–Ca–N4	114.01(6)
N1–Ca–N4	80.86(6)	O1–Ca–N4	144.42(5)
N6–Ca–N4	73.60(6)		

distances (Å) and angles (deg) are provided in Table 1. The monomeric compound **13** has an eight-coordinate calcium core constituting a triangulated dodecahedral geometry. Both chelating ligand L's are tetradentate where the two oxygen atoms and two nitrogen atoms from the same ligand lie

**Figure 2.** ORTEP drawing of the (BDI)₂Ca molecule with thermal ellipsoids drawn at 50% probability level. Hydrogen atoms are omitted for clarity. See also ref 16.**Figure 3.** ORTEP drawing of the Tp^{iPr}CaN(SiMe₃)₂·(THF) molecule with thermal ellipsoids drawn at 30% probability level. Hydrogen atoms are omitted for clarity.

almost on the same plane. Many 8-coordinate calcium complexes with a CaN₄O₄ core have been structurally characterized¹⁷ forming geometries such as square antiprismatic¹⁸ and hexagonal bipyramidal.¹⁹ There is only one example of a structurally characterized calcium complex, bis-(dipyromethenato)calcium, that has a similar dodecahedral geometry to complex **13**.²⁰ The CaN₄ unit in **13** constitutes an elongated tetrahedral geometry with 2 sets of the average N–Ca–N bond angles of 72.30(6)° and 130.53(6)°. The CaO₄ unit has a highly flattened tetrahedral geometry with

- (17) As of August 2003, there are 18 reported calcium complexes with CaN₄O₄ core in Cambridge Crystallographic Data Centre.
 (18) (a) Maumela, H.; Hancock, R. D.; Carlton, L.; Reibenspies, J. H.; Wainwright, K. P. *J. Am. Chem. Soc.* **1995**, *117*, 6698–6707. (b) Kumar, K.; Tweedle, M. F.; Malley, M. F.; Gougoutas, J. Z. *Inorg. Chem.* **1995**, *34*, 6472–6480.
 (19) (a) Chekhlov, A. N. *Koord. Khim.* **2000**, *26*, 163. (b) Akutagawa, T.; Nishihara, S.; Takamatsu, N.; Hasegawa, T.; Nakamura, T.; Inabe, T. *J. Phys. Chem. B* **2000**, *104*, 5871.
 (20) Clarke, E. T.; Squattrito, P. J.; Rudolf, P. R.; Motekaitis, R. J.; Martell, A. E.; Clearfield, A. *Inorg. Chim. Acta* **1989**, *166*, 221–231.

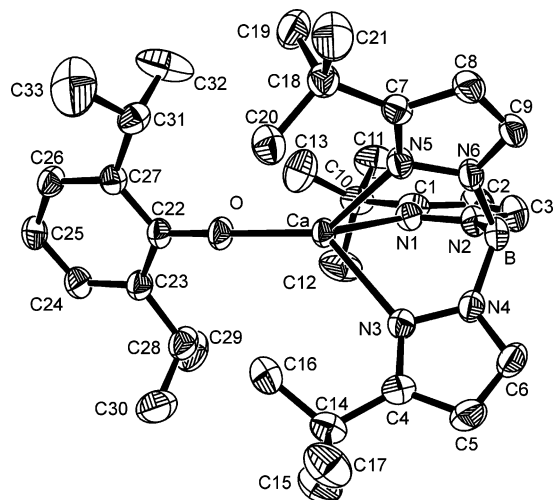


Figure 4. ORTEP drawing of the $\text{Tp}^{\text{iBu}}\text{Ca}(\text{O}-2,6\text{-Pr}_2\text{C}_6\text{H}_3)$ molecule with thermal ellipsoids drawn at 50% probability level. Hydrogen atoms are omitted for clarity.

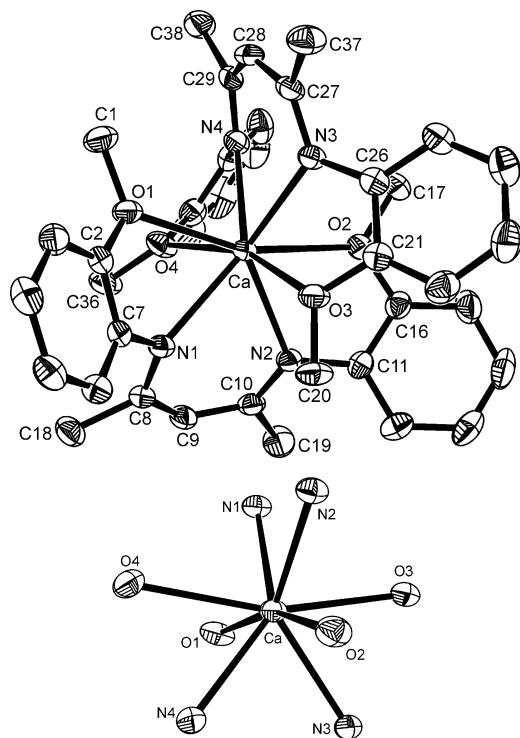


Figure 5. ORTEP drawing of the L_2Ca molecule. Thermal ellipsoids are drawn at 50% probability level. Hydrogen atoms are omitted for clarity. N1, N2, O1, and O2 are from the same ligand. N3, N4, O3, and O4 are from another ligand.

two sets of the average O–Ca–O bond angles of 91.3° and 161.9° . The Ca–O average bond distance is 2.573 \AA , significantly longer than the Mg–O bond distance (2.137 \AA) in a related $(\text{BDI}-\text{OMe})\text{MgN}(\text{SiMe}_3)_2$ compound²¹ where this BDI–OMe ligand binds in an η^4 -manner. The six-membered CaNCCCN rings are highly puckered and the calcium atom sits $1.282(1) \text{ \AA}$ above the plane defined by N1, C9, and N2, and $1.110(1) \text{ \AA}$ above the plane defined by N3, C28, and N4. Unlike $(\text{BDI}-\text{OMe})\text{MgN}(\text{SiMe}_3)_2$ compound where the phenyl rings appear to be almost coplanar

(21) Chisholm, M. H.; Gallucci, J. C.; Phomphrai, K. Manuscript in preparation.

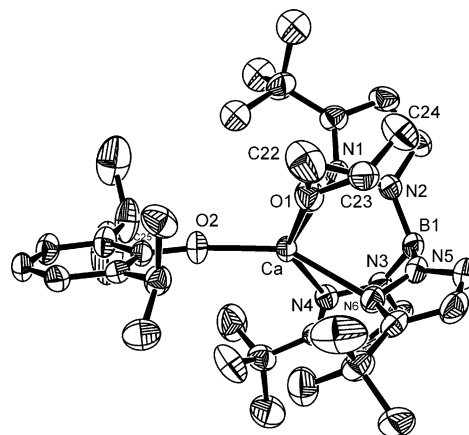


Figure 6. ORTEP drawing of the $\text{Tp}^{\text{iBu}}\text{Ca}(\text{O}-2,6\text{-Pr}_2\text{C}_6\text{H}_3)\cdot(\text{PO})$ molecule with thermal ellipsoids drawn at 50% probability level. Hydrogen atoms are omitted for clarity.

with the backbone NCCCN plane, the average dihedral angle between the phenyl rings and the backbone NCCCN in compound **13** is $60.3(2)^\circ$.

[HB(3-*Bupz*)₃]Ca(O-2,6-Pr₂C₆H₃)·(PO), 14. An ORTEP drawing of the molecular structure of **14** is given in Figure 6 along with selected bond distances (\AA) and angles (deg) in Table 1. Compound **14** is monomeric and calcium is five-coordinate assuming a square pyramidal geometry. Propylene oxide (PO) and three pyrazolyl groups comprise the base of the pyramid. PO coordinates to calcium with the Ca–O_{PO} bond distance of $2.454(2) \text{ \AA}$. The coordination of PO causes a slight lengthening of Ca–O_{aryl} bond distance from $2.106(1)$ in **6** to $2.124(1) \text{ \AA}$, and the average Ca–N bond distances increase from $2.425(1)$ to $2.473(1) \text{ \AA}$. Ca–O2–C25 angle is $167.8(1)^\circ$, a significant deviation from 180° compared to compound **6** ($174.4(1)^\circ$).

A summary of crystallographic data for compounds **1**, **2**, **6**, **13**, and **14** is given in Table 2. Collectively, this work shows that while the β -diiminate ligands $\text{CH}[\text{CMeNC}_6\text{H}_3-2,6\text{-Pr}_2]_2$ and $\text{CH}[\text{CMeNC}_6\text{H}_4-2\text{-OMe}]_2$ may, by virtue of their bulk or chelating $-\eta^4-$ ability, stabilize monomeric Ca(2+) complexes, they can do so only when the other attendant anionic ligand is extremely bulky as in the bis-(trimethylsilyl)amide. Even here, the calcium complexes are capable of undergoing a Schlenk equilibrium to form L_2Ca and $\text{Ca}[\text{N}(\text{SiMe}_3)_2]_2$ complexes. This ligand redistribution is facile upon addition of alcohols and occurs during reactions with lactide (vide infra). Only the use of the extremely bulky Tp ligands stabilizes discrete monomeric calcium complexes and even Tp^{iPr} is evidently not sufficiently bulky as $\text{Ca}(\text{Tp}^{\text{iPr}})_2$ can be formed. We have not found that $\text{Ca}(\text{Tp}^{\text{iBu}})_2$ is formed in any of our reactions.

Reactions with Lactides

(a) Competition Reactions. The compounds $(\text{BDI})\text{ZnN}(\text{SiMe}_3)_2$, $(\text{BDI})\text{MgN}(\text{SiMe}_3)_2$, and $(\text{BDI})\text{CaN}(\text{SiMe}_3)_2\cdot\text{THF}$ allow a direct comparison of the reactivity of the metal–amide bonds in the ring-opening of lactide. In competition experiments, a 1:1 mixture of $(\text{BDI})\text{ZnN}(\text{SiMe}_3)_2$ and $(\text{BDI})\text{MgN}(\text{SiMe}_3)_2$ in benzene-*d*₆ was allowed to react with one equiv of L-lactide. By ^1H NMR spectroscopy, all the

Table 2. Summary of Crystallographic Data of Compound **1**, **2**, **6**, **13**, and **14**

	1	2	6	13	14
empirical formula	C ₃₉ H ₆₇ CaN ₃ OSi ₂ + 0.5 hexane	C ₅₈ H ₈₂ CaN ₄	C ₃₃ H ₅₁ BCaN ₆ O	C ₃₈ H ₄₂ CaN ₄ O ₄	C ₃₆ H ₅₇ BCaN ₆ O ₂
fw	733.30	875.36	598.69	658.84	656.77
color	colorless	colorless	colorless	orange	pale yellow
cryst size (mm)	0.31 × 0.35 × 0.38	0.08 × 0.27 × 0.38	0.27 × 0.27 × 0.31	0.19 × 0.19 × 0.35	0.27 × 0.35 × 0.38
cryst syst	triclinic	monoclinic	monoclinic	monoclinic	monoclinic
space group	<i>P</i> 1	<i>C</i> 2/ <i>c</i>	<i>P</i> 2 ₁ / <i>c</i>	<i>P</i> 2 ₁ / <i>n</i>	<i>P</i> 2 ₁ / <i>n</i>
temp (K)	200	200	200	200	200
<i>a</i> (Å)	11.912(1)	19.513(2)	15.177(1)	11.494(1)	10.482(1)
<i>b</i> (Å)	13.222(1)	12.527(1)	11.737(1)	24.605(3)	20.682(2)
<i>c</i> (Å)	16.888(1)	22.147(2)	20.885(2)	12.313(1)	18.063(2)
α (deg)	70.15(1)				
β (deg)	80.42(1)	100.28(1)	110.69(1)	97.47(1)	101.35(1)
γ (deg)	63.51(1)				
<i>Z</i>	2	4	4	4	4
volume (Å ³)	2238.6(3)	5326.5(8)	3480.3(5)	3452.7(6)	3839.2(7)
density _{calc} (g/cm ³)	1.088	1.092	1.143	1.267	1.136
wavelength (Å)	0.71073	0.71073	0.71073	0.71073	0.71073
abs coeff (mm ⁻¹)	0.226	0.157	0.214	0.227	0.201
θ range (deg)	2.04–27.49	2.07–27.48	2.07–27.49	2.35–25.01	2.21–25.02
reflns collected	47522	46450	60025	47477	38233
independent reflns	10257	6114	7975	6083	6766
R1(F) ^a [<i>I</i> > 2σ(<i>I</i>)]	0.0479	0.0448	0.0406	0.0459	0.0463
R1(F) ^a (all data)	0.0633	0.0635	0.0542	0.0651	0.0569
wR2(F ²) ^a (all data)	0.1362	0.1317	0.1102	0.1377	0.1263
GOF	1.044	1.055	1.040	1.058	1.028

^a R1(F) = Σ||F_o - |F_c||/Σ|F_o|; wR2(F²) = {Σw(F_o² - F_c²)/Σw(F_o²)^{1/2}}; W = 1/[σ²(F_o²) + (xP)² + yP]; P = (F_o² + 2F_c²)/3 where x = 0.0660, y = 0.9247 for **1**; x = 0.0680, y = 2.2133 for **2**; x = 0.0522, y = 1.0612 for **6**; x = 0.0791, y = 1.1756 for **13**; x = 0.0543, y = 2.6477 for **14**.

magnesium complex was consumed (a complete disappearance of MgN(SiMe₃)₂ peak) and none of the zinc complex had reacted. The product is proposed to be a ring-opening complex (BDI)Mg[OCH(Me)C(O)]_nN(SiMe₃)₂ based on an appearance of a new C(O)N(SiMe₃)₂ peak. In a similar experiment, (BDI)CaN(SiMe₃)₂·THF and (BDI)MgN(SiMe₃)₂ were allowed to react with one equivalent of L-lactide and here only the magnesium amide complex remained. Thus, the reactivity of the M–N bonds toward ring-opening of lactide is established to be Ca > Mg > Zn. This correlates well with their reactivity toward chlorinated solvents such as CH₂Cl₂ where the calcium and magnesium complexes react but the zinc complex does not, and, in general, would seem to correlate with the expected degree of ionic or polar character to the M–N bond: M^{δ+}–NR₂^{δ-}.

(b) Polymerization of Lactide. When the compound (BDI)CaN(SiMe₂)₂·THF, **1**, was allowed to react with *rac*-LA, 200 equiv, in THF at room temperature, polymerization to >90% conversion was achieved in 2 h yielding atactic PLA. In contrast, (BDI)MgN(SiMe₃)₂ and 200 equiv *rac*-LA gave ca. 90% heterotactic PLA within 5 min. This reactivity order Mg > Ca in the polymerization of LA is the opposite of that in the competition experiments described above, and probably results from the fact that a complex of the form (BDI)CaOP where OP represents the growing polymer chain is not monomeric or well-defined. Because Ca is bigger than Mg, the BDI ligand is not sufficiently sterically demanding to prevent aggregation or ligand scrambling and the formation of atactic-PLA implies that the reactive site for ring-opening is not sufficiently crowded to impart any stereoselectivity in the ring-opening event. A supporting experiment to this explanation is the fact that when (BDI)CaN(SiMe₃)₂ was allowed to react with one equiv

of HOⁱPr even at –78 °C, (BDI)₂Ca was obtained (probably through a rearrangement of (BDI)CaOⁱPr) as a major product rather than (BDI)CaOⁱPr, suggesting that (BDI)CaOⁱPr (a mimic of the growing polymer species) is not a stable monomeric unit.

The amide complexes with the bulkier Tp ligand set, complexes **3**, **7**, and **9**, were also allowed to react with 200 equiv of *rac*-LA in THF. A similar reaction was carried out with compound **11** which has the chiral 9-BBN–Bp⁽⁺⁾–Cam ligand. The resulting polymers were examined by ¹H NMR spectroscopy and the tacticity was investigated by examination of the methine proton signals with homo-decoupling²² (see Figure 7). In all cases, polymerization of *rac*-LA was very rapid (90% conversion within 5 min) and the Tp^{tBu}-containing complex **3** was extremely rapid (polymerization to >90% in less than 1 min) and stereoselective in producing ca. 90% heterotactic PLA with a PDI of 1.74 (*M*_n = 37.8 kg mol⁻¹). [The sum of *isi* and *sis* tetrad signals constitutes 90% of the total integral of the methine proton signals.]

The complex (Tp^{tBu})Ca(OC₆H₃-2,6-Pr₂)₂·THF, **6**, is also very active in the polymerization of *rac*-LA. In THF, the stereoselectivity and rate of polymerization is similar to that seen for the amide precursor complex **3**. A PDI of 1.68 (*M*_n = 40.1 kg mol⁻¹) was observed and is believed to reflect the relative rate of insertion into the Ca–OAr bond being slower than the subsequent rate of propagation and transesterification.

The Ca–OC₆H₃-2,6-Pr₂ bond in **6** is, unlike the Ca–N amide bond in **3**, inert to CH₂Cl₂ solvent, and so methylenedichloride or CD₂Cl₂ can be used in studies of the

(22) Zell, M. T.; Padden, B. E.; Paterick, A. J.; Thakur, K. A. M.; Kean, R. T.; Hillmyer, M. A.; Munson, E. J. *Macromolecules* **2002**, *35*, 7700–7707.

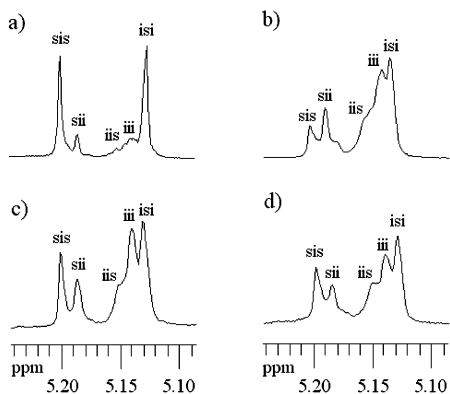


Figure 7. ^1H NMR spectra (CDCl_3 , 400 MHz) of the homodecoupled CH resonance of poly(*rac*-lactide) prepared in THF using (a) $[\text{HB}(3\text{-}^1\text{BuPz})_3]\text{CaN}(\text{SiMe}_3)_2$, **3**; (b) $[\text{HB}(3\text{-}^1\text{Prpz})_3]\text{CaN}(\text{SiMe}_3)_2\cdot(\text{THF})$, **7**; (c) $\text{Tp}^{\text{Men}}\text{CaN}(\text{SiMe}_3)_2$, **9**, and (d) $[(9\text{-BBN})\text{Bp}^{(+)-\text{Cam}}]\text{Ca-N}(\text{SiMe}_3)_2\cdot 2\text{THF}$, **11**, as initiators.

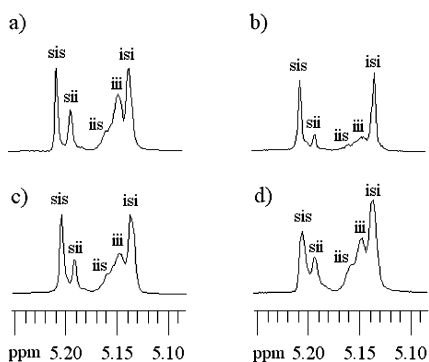


Figure 8. ^1H NMR spectra (CDCl_3 , 400 MHz) of the homodecoupled CH resonance of poly(*rac*-lactide) prepared in (a) CH_2Cl_2 ; (b) THF; (c) *rac*-propylene oxide, and (d) cyclohexene oxide using $[\text{HB}(3\text{-}^1\text{BuPz})_3]\text{Ca}(\text{O-2,6-}^1\text{Pr}_2\text{C}_6\text{H}_3)$, **6**, as an initiator.

polymerization of LA for complex **6**, but not for **3**. In CH_2Cl_2 , less stereoselectivity in polymerization was observed, although the reaction was extremely rapid: >90% within 1 min for polymerization of 200 equiv *rac*-LA. Since the Ca–O bond was unreactive toward PO and cyclohexene oxide, these oxiranes were also employed as solvents in the polymerization of *rac*-LA. The percent of heterotactic tetrads was less than that for THF which leads us to suggest that the degree of heterotacticity in the PLA correlates with the coordinating ability of the solvent as a ligand to calcium: $\text{THF} > \text{PO} \approx \text{CHO} > \text{CH}_2\text{Cl}_2$ (Figure 8).

Conclusions

This work provides the first examples of the synthesis and characterization of monomeric heteroleptic calcium amide and alkoxide complexes for the ring-opening polymerization of lactides. Although monomer β -diiminate precursors can be prepared, their use in polymerization is limited by ligand scrambling reactions. A better ligand system is shown to be the tridentate trispyrazolyl borates. Even here, the use of bulky substituent as seen in the Tp^{iBu} ligand is necessary to confer single-site living polymerization behavior and stereoselectivity in the ring-opening event. Interestingly, the less sterically demanding Tp^{iPr} ligand does not confer any stereocontrol. For a series of compounds Tp^{iBu} MOR, the reactivity order is $\text{M} = \text{Ca} > \text{Mg} > \text{Zn}$ and the calcium

complexes **3** and **6** reported here are probably the most reactive and stereoselective catalysts reported to date. Further investigation of the polymerizing properties of the compounds will be undertaken.

In view of the importance of steric hindrance and the coordinating ability of the solvent in controlling both catalyst stability and polymer tacticity, we are proceeding toward the development of Tp ligands incorporating ether groups; e.g., in place of ^tBu substituents, we will have $\text{Me}_2\text{CCH}_2\text{OMe}$ groups. The hemilabile ether ligands could confer kinetic persistence to the catalyst system even in the presence of trace amounts of water. An ideal calcium catalyst would be of the form LCaOH where L is a polydentate ligand capable of stabilizing the hydroxide ligand with respect to oxo-bridge formation.

Finally, it is worth noting that the complexes reported here are active to ROP of lactide but not to PO or CHO. This adds further support to the conclusion that this *cis*-migratory ring-opening of PO is not operative for the coordinate anionic polymerization of PO.²³ The calcium–PO complex, **14**, is a rare example of a structurally characterized PO–metal complex²⁴ and quite striking inasmuch as calcium is commonly used in the industrial production of polypropyleneoxide.

Experimental Section

General Considerations. The manipulation of air-sensitive compounds involved the use of anhydrous solvents and dry and oxygen-free nitrogen employing standard Schlenk line and drybox techniques. *Rac*-lactide was purchased from Aldrich and was sublimed three times prior to use. Tetrahydrofuran, dichloromethane, hexanes, and toluene were distilled under nitrogen from sodium/benzophenone, calcium hydride, potassium metal, and sodium metal, respectively. The β -diiminate ligands LH, where $\text{L} = \text{CH}[\text{CMeNC}_6\text{-H}_3\text{-2,6-Pr}_2]_2$ ²⁵ and $\text{CH}[\text{CMeNC}_6\text{H}_4\text{-2-OMe}]_2$,²⁶ $[\text{HB}(3\text{-}^1\text{BuPz})_3]\text{K}$,²⁷ $[\text{HB}(3\text{-}^1\text{Prpz})_3]\text{K}$,²⁸ $[\text{HB}(3\text{-}^1\text{Phpz})_3]\text{K}$,²⁷ $\text{Tp}^{\text{Men}}\text{Ti}$,²⁹ and $[(9\text{-BBN})\text{Bp}^{(+)-\text{Cam}}]\text{K}$ ³⁰ were prepared according to literature procedures. $\text{KN}(\text{SiMe}_3)_2$, 2,6-diisopropylphenol, TIOAc, and CaI_2 were purchased from Aldrich and used as received.

Measurements. ^1H (400.1 MHz) and $^{13}\text{C}\{^1\text{H}\}$ (100.6 MHz) spectra were recorded in C_6D_6 and toluene- d_8 on Bruker DPX-400 NMR spectrometer and were referenced to the residual protio impurity peak (C_6D_6 , δ 7.15; toluene- d_8 , 2.09 for ^1H and, C_6D_6 , δ

- (23) Antelmann, B.; Chisholm, M. H.; Iyer, S. S.; Huffman, J. C.; Navarro-Llobet, D.; Pagel M. *Macromolecules* **2001**, *34*, 3159.
 (24) (a) Beckwith, J. D.; Tschinski, M.; Picot, A.; Tsunoda, M.; Bachman, R.; Gabbai, F. P. *Organometallics* **2001**, *20*, 3169. (b) Darenbourg, D. J.; Holtcamp, M. W.; Khandelwal, B.; Klausmeyer, K. K.; Reibenspies, J. H. *J. Am. Chem. Soc.* **1995**, *117*, 538. (c) Harder, S.; Boersma, J.; Brandsma, L.; Kanters, J. A.; Duisenberg, A. J. M.; van Lenthe, J. H. *Organometallics* **1990**, *9*, 511.
 (25) Feldman, J.; McLain, S. J.; Parthasarathy, A.; Marshall, W. J.; Calabrese, J. C.; Arthur, S. D. *Organometallics* **1997**, *16*, 1514–1516.
 (26) Carey, D. T.; Cope-Eatough, E. K.; Vilaplana-Mafé, E.; Mair, F. S.; Pritchard, R. G.; Warren, J. E.; Woods, R. J. *J. Chem. Soc., Dalton Trans.* **2003**, 1083–1093.
 (27) Trofimenko, S.; Calabrese, J. C.; Thompson, J. S. *Inorg. Chem.* **1987**, *26*, 1507–1514.
 (28) Trofimenko, S.; Calabrese, J. C.; Domaille, P. J.; Thompson, J. S. *Inorg. Chem.* **1989**, *28*, 1091–1101.
 (29) LeCloux, D. D.; Tokar, C. J.; Osawa, M.; Houser, R. P.; Keyes, M. C.; Tolman, W. B. *Organometallics* **1994**, *13*, 2855–2866.
 (30) Chisholm, M. H.; Iyer, S. S.; Streib, W. E. *New. J. Chem.* **2000**, *24*, 393–398.

128.0; toluene- d_8 , 20.4 for $^{13}\text{C}\{^1\text{H}\}$). Elemental analyses were done by Atlantic Microlab, Inc. Gel permeation chromatography measurements were carried out using a Waters 1525 binary HPLC pump and a Waters 410 differential refractometer equipped with styragel HR 2&4 columns (100 and 10 000 Å). The GPC was eluted with THF at 35 °C running at 1 mL/min and was calibrated using polystyrene standard.

(BDI)CaN(SiMe₃)₂·(THF), 1. A 15-mL portion of THF was added to a mixture of the β -diimine ligand (BDI)H (0.250 g, 0.598 mmol) and KN(SiMe₃)₂ (0.238 g, 1.19 mmol). After the mixture was stirred for 1 h, it was added to a slurry of Ca₂ (0.176 g, 0.599 mmol) in 5 mL THF and stirred overnight. After filtration, the volatile components were removed under dynamic vacuum giving compound **1** (0.33 g, 80%). Crystals suitable for single-crystal X-ray crystallography were obtained by placing a concentrated hexanes solution in a freezer overnight. CCDC number: 192310. MS (EI): $m/z = 617.4$ (M - THF)⁺. Anal. Calcd for C₃₉H₆₇N₃Si₂O: C, 67.92; H, 9.71; N, 6.09. Found: C, 67.02; H, 9.33; N, 5.88. ¹H NMR (C₆D₆, 400 MHz): 7.20–7.10 (m, 6H, Ar-H), 4.85 (s, 1H, β -CH), 3.37 (m, 4H, O(CH₂CH₂)₂), 3.25 (sept, 4H, CHMe₂), 1.69 (s, 6H, α -CH₃), 1.36 (d, 12H, CHMe₂), 1.26 (d, 12H, CHMe₂), 1.11 (m, 4H, O(CH₂CH₂)₂), 0.20 (s, 18H, SiMe₃). ¹³C{¹H} NMR (C₆D₆): 166.48 (C=N), 147.36 (*ipso*-C), 141.50 (*o*-C), 124.65 (*p*-C), 124.11 (*m*-C), 94.13 (β -C), 69.22 (O[CH₂CH₂]₂), 28.50 (CHMe₂), 25.48 (CHMe₂), 25.22 (α -Me), 24.92 (O[CH₂CH₂]₂), 24.79 (CHMe₂), 5.99 (SiMe₃).

(BDI)₂Ca, 2. The synthesis of CaL₂ follows the preparation for compound **1** except that 2 equiv of LH (0.500 g, 1.19 mmol) were used giving CaL₂ (0.39 g, 75%). Crystals suitable for single-crystal X-ray crystallography were obtained by placing a concentrated hexanes solution in a freezer. CCDC number: 192311. Anal. Calcd for C₅₈H₈₂N₄Ca: C, 79.64; H, 9.37; N, 6.41. Found: C, 79.35; H, 9.33; N, 6.40. ¹H NMR (C₆D₆): 7.25–6.80 (m, 12H, Ar-H), 4.93 (s, 2H, β -CH), 3.17 (sept, 2H, CHMe₂), 2.99 (sept, 4H, CHMe₂), 2.60 (sept, 2H, CHMe₂), 1.82 (s, 6H, α -CH₃), 1.54 (s, 6H, α -CH₃), 1.49, 1.29, 1.24, 1.19, 1.01, 0.97, 0.50, 0.46 (d, 6H each, CHMe₂).

[HB(3-^tBupz)₃]CaN(SiMe₃)₂, 3. A 15-mL aliquot of THF was added to a mixture of [HB(3-^tBupz)₃]K (0.300 g, 0.714 mmol), Ca₂ (0.210 g, 0.715 mmol), and KN(SiMe₃)₂ (0.142 g, 0.712 mmol). The cloudy white mixture was then stirred overnight and filtered. Any volatile components were removed under dynamic vacuum and the product was redissolved in 15 mL of benzene. After filtration and subsequent solvent removal, the product was obtained as a white solid (0.29 g, 70%). Anal. Calcd for C₂₇H₅₂N₇-BSi₂Ca: C, 55.78; H, 8.94; N, 16.86. Found: C, 55.01; H, 8.97; N, 16.54. ¹H NMR (C₆D₆): 7.41 (d, 3H, 5-H), 5.80 (d, 3H, 4-H), 1.35 (s, 27H, ^tBu), 0.34 (s, 18H, SiMe₃). ¹³C{¹H} NMR (C₆D₆): 164.79 (3-C), 138.69 (5-C), 101.81 (4-C), 32.38 (CMe₃), 31.66 (CMe₃), 5.93 (SiMe₃).

[HB(3-^tBupz)₃]CaI·(THF), 4. A solution of [HB(3-^tBupz)₃]Ti (0.500 g, 0.854 mmol) in 15 mL of THF was added dropwise to a slurry of Ca₂ (0.251 g, 0.854 mmol) in 10 mL of THF. The resulting yellow mixture was then stirred for 1 h and filtered. Any volatile components were removed under dynamic vacuum and the product was redissolved in 15 mL of benzene. After filtration and subsequent solvent removal, the product was obtained as a white solid (0.44 g, 83%). Anal. Calcd for C₂₅H₄₂N₆BIOCa: C, 48.42; H, 6.77; N, 13.55. Found: C, 48.11; H, 6.53; N, 13.44. ¹H NMR (C₆D₆): 7.44 (d, 3H, 5-H), 5.82 (d, 3H, 4-H), 3.17 (m, 4H, O(CH₂-CH₂)₂), 1.38 (s, 27H, ^tBu), 1.05 (m, 4H, O(CH₂CH₂)₂).

[HB(3-^tBupz)₃]Ca(O-2,6-ⁱPr₂C₆H₃)·(THF), 5. A 15-mL aliquot of THF was added to a mixture of [HB(3-^tBupz)₃]K (0.300 g, 0.714 mmol), Ca₂ (0.210 g, 0.715 mmol), and KN(SiMe₃)₂ (0.142 g,

0.712 mmol). The cloudy white mixture was then stirred overnight. 2,6-Diisopropylphenol (0.134 mL, 0.720 mmol) was added dropwise to the resulting mixture. The white mixture was stirred for 2 h and filtered. Any volatile components were removed under dynamic vacuum and the product was redissolved in 15 mL benzene. After filtration and subsequent solvent removal, the product was obtained as a white solid (0.34 g, 71%). Anal. Calcd for C₃₇H₅₉N₆O₂BCa: C, 66.30; H, 8.80; N, 12.54. Found: C, 65.55; H, 9.11; N, 12.75. ¹H NMR (C₆D₆): 7.49 (d, 3H, 5-H), 7.33 (d, 2H, *m*-ArH), 7.00 (t, 1H, *p*-ArH), 5.86 (d, 3H, 4-H), 3.90 (br, 2H, CHMe₂), 3.22 (br, 4H, O(CH₂CH₂)₂), 1.41 (d, 12H, CHMe₂), 1.31 (s, 27H, ^tBu), 1.14 (br, 4H, O(CH₂CH₂)₂). ¹³C{¹H} NMR (C₆D₆): 165.14 (3-C), 137.99 (5-C), 136.26 (*o*-C), 123.24 (*m*-C), 101.68 (4-C), 68.40 (O[CH₂-CH₂]₂), 32.04 (CMe₃), 31.12 (CMe₃), 26.54 (CHMe₂), 25.38 (CHMe₂), 25.23 (O[CH₂CH₂]₂).

[η^3 -HB(3-^tBupz)₃]Ca(O-2,6-ⁱPr₂C₆H₃), 6. Compound **5** (0.500 g, 0.746 mmol) was heated to 150 °C under vacuum for 1 h giving compound **6** in quantitative yield. Crystals suitable for single-crystal X-ray crystallography were obtained by placing a concentrated toluene solution in a freezer overnight. CCDC number: 192309. Anal. Calcd for C₃₃H₅₁N₆BOCa: C, 66.25; H, 8.52; N, 14.05. Found: C, 66.24; H, 8.57; N, 14.06. ¹H NMR (C₆D₆): 7.44 (d, 3H, 5-H), 7.32 (d, 2H, *m*-ArH), 7.00 (t, 1H, *p*-ArH), 5.80 (d, 3H, 4-H), 3.81 (sept, 2H, CHMe₂), 1.39 (d, 12H, CHMe₂), 1.27 (s, 27H, ^tBu). ¹³C{¹H} NMR (C₆D₆): 165.41 (3-C), 138.04 (5-C), 136.05 (*o*-C), 123.10 (*m*-C), 101.65 (4-C), 32.02 (CMe₃), 31.18 (CMe₃), 26.98 (CHMe₂), 24.92 (CHMe₂).

[η^3 -HB(3-ⁱPrpz)₃]CaN(SiMe₃)₂·THF, 7. THF (15 mL) was added to a mixture of [HB(3-ⁱPrpz)₃]K (0.270 g, 0.713 mmol), Ca₂ (0.210 g, 0.715 mmol), and KN(SiMe₃)₂ (0.142 g, 0.712 mmol). The cloudy white mixture was then stirred overnight and filtered. Any volatile components were removed under dynamic vacuum and the product was redissolved in 15 mL of benzene. After filtration and subsequent solvent removal, the product was obtained as a white solid (0.31 g, 71%). Crystals suitable for single-crystal X-ray crystallography were obtained by placing a concentrated THF solution in a freezer. Anal. Calcd for C₂₈H₅₄N₇Si₂OBCa: C, 55.00; H, 8.83; N, 16.04. Found: C, 54.52; H, 8.66; N, 16.40. ¹H NMR (C₆D₆): 7.50 (d, 3H, 5-H), 5.87 (d, 3H, 4-H), 3.57 (m, 4H, O(CH₂-CH₂)₂), 3.41 (br, 3H, CHMe₂), 1.26 (m, 4H, O(CH₂CH₂)₂), 1.19 (d, 18H, CHMe₂), 0.41 (s, 18H, SiMe₃). ¹³C{¹H} NMR (C₆D₆): 162.14 (3-C), 137.87 (5-C), 100.25 (4-C), 69.44 (O[CH₂CH₂]₂), 28.23 (CHMe₂), 25.18 (O[CH₂CH₂]₂), 24.53 (CHMe₂), 6.00 (SiMe₃).

[HB(3-Phpz)₃]Ca, 8. The synthesis follows the procedure for the preparation of compound **3** but employs [HB(3-Phpz)₃]K (0.343 g, 0.714 mmol), giving compound **8** (0.30 g, 85%). Anal. Calcd for C₅₄H₄₄N₁₂B₂Ca: C, 70.32; H, 4.77; N, 18.22. Found: C, 70.47; H, 4.90; N, 18.33. ¹H NMR (C₆D₆): 7.74 (d, 6H, 5-H), 7.27 (d, 12H, ArH), 6.70 (t, 6H, ArH), 6.50 (t, 12H, ArH), 6.10 (d, 6H, 4-H), 3.57 (m, 4H, O(CH₂CH₂)₂), 1.40 (m, 4H, O(CH₂CH₂)₂).

[HB((7R)-ⁱPr-(4R)-Me-4,5,6,7-tetrahydro-2H-indazolyl)₃]CaN(SiMe₃)₂ or Tp^{Men}CaN(SiMe₃)₂, 9. A solution of Tp^{Men}Ti (0.740 g, 0.990 mmol) in 10 mL benzene was added dropwise to a solution of Ca[N(SiMe₃)₂]₂·2THF (0.500 g, 0.990 mmol) in 10 mL of benzene. The solution was stirred for 30 min and then stripped to dryness giving a mixture of **9** and TiN(SiMe₃)₂. TiN(SiMe₃)₂ is removed by sublimation at 90 °C to a coldfinger at 10⁻² Torr. The resulting solid was then redissolved in 15 mL of benzene. After filtration and subsequent solvent removal, the product was obtained as a white solid (0.45 g, 61%). ¹H NMR (C₆D₆): 7.36 (s, 3H), 2.87 (m, 3H), 2.47 (m, 3H), 2.14 (m, 3H), 1.81 (m, 3H), 1.43–1.62 (m, 9H), 1.17 (d, 9H), 1.02 (m, 9H), 0.87 (m, 9H), 0.40 (s, 18H, SiMe₃).

Tp^{Men}CaI·(THF), 10. A solution of Tp^{Men}TI (0.641 g, 0.854 mmol) in 15 mL THF was added dropwise to a slurry of CaI₂ (0.251 g, 0.854 mmol) in 10 mL of THF. The resulting yellow mixture was then stirred for 1 h and filtered. Any volatile components were removed under dynamic vacuum and the product was redissolved in 15 mL of benzene. After filtration and subsequent solvent removal, the product was obtained as a white solid (0.52 g, 77%). ¹H NMR (C₆D₆): 7.44 (s, 3H), 3.58 (m, 4H, THF), 2.80–2.93 (m, 3H), 2.46–2.60 (m, 3H), 2.26–2.38 (m, 3H), 2.12–2.26 (m, 3H), 1.70–1.82 (m, 3H), 1.43–1.60 (m, 6H), 1.23 (m, 4H, THF), 1.18 (d, 9H), 1.07 (d, 9H), 0.81 (d, 9H).

[(Cyclooctane-1,5-diy)bis[(4S,7R)-7,8,8-trimethyl-4,5,6,7-tetrahydro-4,7-methano-2H-indazol-2-yl]borato]CaN(SiMe₃)₂·2THF or [(9-BBN)Bp^{(+)-Cam}]CaN(SiMe₃)₂·2THF, 11. THF (15 mL) was added to a mixture of [(9-BBN)Bp^{(+)-Cam}]K (0.364 g, 0.714 mmol), CaI₂ (0.210 g, 0.715 mmol), and KN(SiMe₃)₂ (0.142 g, 0.712 mmol). The cloudy white mixture was then stirred overnight and filtered. Any volatile components were removed under dynamic vacuum and the product was redissolved in 15 mL of benzene. After filtration and subsequent solvent removal, the product was obtained as a white solid (0.44 g, 76%). ¹H NMR (C₆D₆): 7.34 (s, 2H), 3.72 (m, 8H, THF), 1.95–2.25 (m, 10H), 1.78–1.95 (m, 2H), 1.50–1.70 (m, 6H), 1.35–1.45 (m, 12H), 1.27 (s, 6H), 0.74 (s, 6H), 0.42 (s, 18H, SiMe₃).

LCaN(SiMe₃)₂·(THF), 12, where L = CH[CMeN(C₆H₄-2-OMe)₃. A solution of LH (0.500 g, 1.61 mmol) in 10 mL of benzene was added dropwise to a solution of Ca[N(SiMe₃)₂]₂·2THF (0.813 g, 1.61 mmol) in 5 mL of benzene and stirred for 10 min. The resulting mixture was then stripped to dryness giving an orange solid (0.84 g, 90%). ¹H NMR (C₆D₆): 6.70–6.80 (m, 4H, ArH), 6.60–6.70 (m, 4H, ArH), 5.07 (s, 1H, β-CH), 3.84 (s, 6H, OMe), 3.40 (m, 4H, O(CH₂CH₂)₂), 2.03 (s, 6H, α-Me), 1.15 (m, 4H, O(CH₂CH₂)₂), 0.39 (s, 18H, SiMe₃).

L₂Ca, 13, where L = CH[CMeNC₆H₄-2-OMe]₂. A solution of LH (0.500 g, 1.61 mmol) in 10 mL of benzene was added to a solution of Ca[N(SiMe₃)₂]₂·2THF (0.406 g, 0.805 mmol) at room temperature. The resulting solution was stirred for 15 min and stripped to dryness giving an orange solid in quantitative yield. Crystals suitable for single-crystal X-ray crystallography were obtained by placing a concentrated hexanes solution in a freezer. CCDC number: 217757. Anal. Calcd for C₃₈H₄₂N₄O₄Ca: C, 69.31; H, 6.38; N, 8.51. Found: C, 68.92; H, 6.26; N, 8.34. ¹H NMR (C₆D₆): 6.60–7.00 (m, 12H, ArH), 6.32 (d, 4H, *J* = 7.9 Hz, ArH), 4.89 (s, 2H, β-CH), 3.48 (s, 12H, OMe), 2.02 (s, 12H, α-Me).

[HB(3-ⁱBupz)₃]Ca(O-2,6-ⁱPr₂C₆H₃)·(PO), 14. *Rac*-propylene oxide (0.500 mL, 7.15 mmol) was added to a solution of compound **6** (0.300 g, 0.501 mmol) in 10 mL of hexanes. The hexanes solution was then carefully concentrated, and crystals suitable for single-crystal X-ray crystallography were obtained by placing the concentrated solution in a freezer (0.14 g, 43%). CCDC number: 217761. ¹H NMR (C₆D₆): 7.48 (d, 3H, 5-H), 7.32 (d, 2H, *m*-ArH),

6.97 (t, 1H, *p*-ArH), 5.85 (d, 3H, 4-H), 3.89 (sept, 2H, CHMe₂), 2.52 (m, 1H, CH), 2.27 (dxd, 1H, CH₂), 1.95 (dxd, 1H, CH₂), 0.92 (d, 3H, CH₃), 1.38 (d, 12H, CHMe₂), 1.31 (s, 27H, ^tBu).

General Polymerization Procedure. *Rac*-lactide (0.500 g, 3.47 mmol) was dissolved in 6.0 mL of CH₂Cl₂ or THF. A solution of the corresponding catalyst precursor (0.0174 mmol) in 1.5 mL of CH₂Cl₂ or THF was then added to the lactide solution (200:1 [lactide]/[catalyst]). The reaction was stirred at room temperature for the desired time, after which small aliquots were taken to monitor the conversion. When the conversion was greater than 90%, the polymerization was quenched with excess methanol. The polymer precipitate was then filtered and dried under vacuum to constant weight.

X-ray Crystallography. Single-crystal X-ray diffraction data were collected on a Nonius Kappa CCD diffractometer at low temperature using an Oxford Cryosystems Cryostream cooler. Crystals were coated with oil prior to being placed in the nitrogen gas stream. The data collection strategy was set up to measure a hemisphere of reciprocal space for compound **1**, a quadrant for **2**, **6**, **13**, and **14** with a redundancy factor of 2.2, 4.0, 4.0, 4.3, and 2.8, which means that 90% of the reflections were measured at least 2.2, 4.0, 4.0, 4.3, and 2.8 times, respectively. A combination of φ and ω scans with a frame width of 1.0° was used. Data integration was done with Denzo.³¹ Scaling and merging of the data was done with Scalepack.³¹ The structures were solved by either the Patterson method or direct methods in SHELXS-86.³² Full-matrix least-squares refinements based on F² were performed in SHELXL-93.³³ The methyl group hydrogen atoms were added at calculated positions using a riding model with U(H) = 1.5*Ueq (bonded C atom). For each methyl group, the torsion angle which defines its orientation about the C–C bond was refined. The other hydrogen atoms were included in the model at calculated positions using a riding model with U(H) = 1.2*Ueq (bonded C atom). Neutral atom scattering factors were used and include terms for anomalous dispersion.³⁴

Acknowledgment. We thank the Department of Energy, Office of Basic Sciences, Chemistry Division, for support of this work.

Supporting Information Available: Crystallographic data for compounds **1**, **2**, **6**, **13**, and **14** (cif). This material is available free of charge via the Internet at <http://pubs.acs.org>.

IC0490730

(31) Otwinowski, Z.; Minor, W. *Macromolecular Crystallography*, Part of the series Methods in Enzymology, Vol. 276, Carter, C. W., Jr.; Sweet, R. M. Eds.; Academic Press: San Diego, CA, 1997; part A, pp 307–326.

(32) Sheldrick, G. M. *Acta Crystallogr.* **1990**, *A46*, 467–473.

(33) Sheldrick, G. M. Universität Göttingen, Germany, 1993.

(34) *International Tables for Crystallography*; Hahn, T., Ed.; Kluwer Academic Publishers: Dordrecht, The Netherlands, 1992.